Geologie en Mijnbouw **75:** 269–274, 1996.

Neutron activation analysis of trace elements in the Geulhemmerberg Cretaceous/Tertiary boundary section, SE Netherlands

J. Smit[1] & R. Rocchia[2]
[1] *Institute of Earth Sciences, Vrije Universiteit, de Boelelaan 1085, 1081 HV Amsterdam, the Netherlands;*
[2] *Centre des Faibles Radioactivités, lab mixte CEA-CNRS, ave. la Terrasse, 91198 Gif-sur-Yvette cedex, France*

Received 24 October 1995; accepted in revised form 9 May 1996

Key words: INAA, iridium, K/T boundary

Abstract

The Geulhemmerberg K/T boundary section was analysed for (trace) elements by instrumental neutron activation analysis (INAA). Twenty-seven elements were detected in almost all of the 22 samples. Another seven elements were above detection limit in only a few samples, and four elements were below the detection limit in all samples. Anomalous Ir levels have not been found in any sample. However, when Th-normalized, there is an indication for higher concentrations of Ir (and Cr) just below the K/T boundary, possibly due to downward diffusion. The distributions of most trace elements can be explained by the alternation of layers of clay and almost pure limestone in the section, and by the lithophile, chalcophile or siderophile character of the elements. Strontium, usually correlating positively with Ca and $CaCO_3$, correlates negatively with Ca in the Geulhemmerberg section. The relatively high values of Sr in the clay-layers indicate that these layers were shielded from diagenesis. The La/Ce ratio is lower in the clay than in the limestone layers. This may reflect dysoxic conditions in seawater during the deposition of the clay layers. The La/Yb ratio is low in the uppermost Maastrichtian, and high in the basal Danian. An enrichment of Co and Fe at the Berg en Terblijt hardground can be explained by the presence of iron encrustations.

Introduction

Instrumental neutron activation analysis (INAA) has successfully been applied to detect anomalous iridium concentrations at the Cretaceous/Tertiary (K/T) boundary worldwide (Alvarez et al. 1980; Alvarez and Asaro 1990; Smit and Hertogen 1980). The number of K/T boundary sites in which the Ir anomaly has been observed, is now well over 140, and still growing. In effect, not a single K/T boundary section is known where this anomaly has not been found, with the exception of those sections where a considerable hiatus exists at the K/T boundary. Because the Ir anomaly coincides with the K/T boundary in its stratotype at El Kef, Tunisia, and because of its global occurrence, it has become a prime marker for the K/T boundary, supplementing biostratigraphy.

Twenty-two samples from the standard sample-set across the Berg en Terblijt Horizon in the Geulhemmerberg section were subjected to INAA (IG1–22, Figure 1; see Brinkhuis and Smit, this issue). One split was analysed for 38 elements according to the methods in use at the Interuniversitary Reactor Institute (IRI) at Delft, the Netherlands (Smit and Ten Kate 1982). Another split was analysed for Ir by coincidence-INAA at the Centre des Faibles Radioactivités, Gif-sur-Yvette, France. Of these 38 elements, 33 are listed in Table 1. The other five are below detection limit in almost all samples. The Ir concentrations were measured with a γ-γ spectrometer detecting in coincidence the 316 and 468 KeV γ-ray lines produced by the decay of ^{192}Ir (Rocchia et al. 1990). The detection limit of Ir is 2 to 8 ng/g at IRI in Delft, and 0.02 ng/g in the coincidence-INAA method at Gif-sur-Yvette.

Tabel 1. Instrumental Neutron Activation of trace elements in the Geulhemmerberg K/T boundary section.

Sample	CaCO3 (%)	Na	K (%)	Ca (%)	Sc	Cr	Fe (%)	Co	Ni	Zn	As	Se	Br	Rb	Sr	Zr	Mo
IG1	98.30	268		41.0	0.29	19.4	0.12	0.39			1.47		1.25	2.27	554		
IG2	98.10	229	0.06	41.1	0.28	21.0	0.34	0.32		2.58	11.50		1.00	3.31	510		6.93
IG3	99.50	268		40.2	0.30	18.4	0.17	0.23		2.57	3.71		1.00	1.52	545		
IG4	95.60	330	1.26	37.3	0.50	17.6	0.41	0.80		3.77	8.11		0.93	6.60	614		
IG5	95.20	314		37.8	0.71	18.0	0.50	1.18		8.20	11.10		1.33	8.62	578	23.40	
IG6*A1	83.90	455	0.38	36.4	2.05	49.6	0.74	0.91		13.00	13.30		1.83	25.40	818	41.00	
IG7*A2	68.60	609	0.59	29.5	3.85	85.2	1.36	1.40	27.4	19.60	12.20	0.58	2.05	55.40	1220	95.80	5.21
IG8	85.90	540	0.26	33.3	1.82	47.9	1.01	1.07		14.50	18.00		1.66	23.30	959		13.10
IG9*B	63.80	705	0.55	27.5	4.35	93.7	1.34	1.55		20.60	9.56		2.10	61.40	1330		
IG10*	73.70	570	0.58	31.5	3.32	66.3	1.09	1.25		14.90	12.10		1.61	46.40	1000	41.40	
IG11*C	67.80	652	0.69	28.2	4.25	86.9	1.29	1.63		21.50	11.70		2.21	58.20	1190		
IG12	97.20	334		40.9	0.59	21.5	0.46	0.54			10.20		1.19	5.37	610	22.60	
IG13	94.20	261	0.12	35.1	0.80	26.3	0.59	1.02			11.50		0.86	8.79	508		
IG14*D2	56.40	643	0.80	23.0	4.97	94.5	1.79	2.05		44.00	12.90		2.01	71.40	1060	82.90	
IG15	84.80	488		35.0	1.82	38.9	1.08	2.13		11.60	18.00	0.62	1.62	22.50	969		
IG16*E	57.50	659	0.66	24.9	4.81	81.5	1.61	3.30		27.10	5.76		1.96	66.40	1160	84.90	
IG17*E	58.40	822	0.76	26.9	5.09	83.9	1.40	2.37		29.90	3.69	1.10	3.56	70.80	1610	110.00	
IG18*F	66.20	684	0.64	29.5	3.87	69.5	1.13	1.29		31.50	7.88		2.70	52.70	1320	63.30	
IG19	76.90	551	0.46	31.9	2.21	39.5	0.63	1.14		18.50	2.44	2.36	1.72	31.20	1080		
IG20*G1	61.90	617	0.53	26.7	3.48	64.5	1.34	1.98	33.2	36.70	10.10		1.88	51.30	1210	49.50	
IG21*G2	52.20	568	0.53	23.4	3.52	69.7	1.23	1.46		45.70	10.60	7.00	2.35	48.50	1030		
IG22	69.00	365	0.39	30.4	1.69	40.8	0.78	1.29		30.30	13.30	4.69	1.49	21.50	657	27.60	
error (mean%)	2	3.6	17.9	5.9	3.9	2.8	2.0	5.6	25.0	13.5	5.8	19.0	10.0	10.1	4.7	26.7	38.7
error (range %)		2.7-6.6	9-43	5.1-8.3	1.2-9.3	1.8-4.6	1.5-2.5	1.3-10	20-30	4.8-32	3.1-13	4.4-39	6.1-17	3.7-28	2.9-8.7	13-45	26-49

Values in µg/g, unless where indicated otherwise. Analyses performed at IRI, Delft, except for Ir, which was analysed by R. Rocchia (Centre des Faibles Radioactivités, Gif-sur-Yvette). Errors given as mean and range for all analyses. Blanks = below detection limit. Asterisks * indicate clay samples and are followed by clay layer number. Continued next page.

Results

Iridium

The Ir contents of the 22 samples are below the detection limit in the Delft data-set. The Ir concentrations as measured in Gif-sur-Yvette, are less than 0.05 ng/g in the clay layers, and close to or below the detection limit in the other samples (Table 1). As shown in Figure 1, no distinct Ir anomaly occurs in the Geulhemmerberg section. However, the Th-normalized Ir values are slightly higher in the uppermost Maastrichtian (samples IG1–3), than in the overlying Danian.

Other trace elements

Except for Ir, 32 (trace)elements were detected at IRI in Delft. The concentrations are presented in Table 1. Usually, such concentrations are plotted as 100% carbonate-free in order to allow a useful comparison between the Ca-poor (clay) and the Ca-rich (limestone) layers, and detection of an elemental anomaly. However, the elemental concentrations can also be normalized to a lithophile element which is known to correlate well with the clay content, measured as the insoluble residue, such as Al, Sc, Cs, the rare earth elements (REE), Hf, and Th.

Thorium has been used here (Figure 1) as normalizing element instead of carbonate-free concentrations, because Th couples a strong negative correlation coefficient with $CaCO_3$ ($r = -0.93$, Table 2) to the smallest analytical error in the Geulhemmerberg material (Table 1). Previous INAA analyses of K/T sequences have also shown that Th correlates positively with clay content and Al in carbonate-rich sedimentary rocks (Smit and Ten Kate 1982). Both normalizing methods result in slightly different profiles, probably because the Th and carbonate contents have been analysed on different splits of the samples.

Tabel 1. Continued.

Sample	Sb	Cs	Ba	La	Ce	Nd	Sm	Eu	Tb	Yb	Lu	Hf	Ta	W	Ir (pg/g)	(error) (%)	Th	U
IG1	0.09	0.30		2.02	2.77		0.28	0.08	0.05	0.16	0.02	0.03			18	16.7	0.57	1.60
IG2	0.49	0.28		1.69	2.43		0.25	0.07	0.04	0.15	0.02	0.02			21	14.3	0.52	1.82
IG3	0.17	0.24		1.95	2.90		0.34	0.09	0.04	0.16	0.02	0.14			13	15.4	0.59	1.51
IG4	0.36	0.90		2.65	3.76		0.35	0.10	0.05	0.17	0.02	0.21		0.50	18	83.3	0.71	1.76
IG5	0.35	1.37		3.53	5.82		0.53	0.14	0.09	0.20	0.03	0.22	0.08		20	100.0	1.03	2.10
IG6*A1	0.54	4.29	30.60	6.64	11.80		1.03	0.23	0.13	0.39	0.06	0.62	0.17		15	100.0	2.29	2.57
IG7*A2	0.70	8.79	40.40	9.63	17.50		1.53	0.28	0.19	0.65	0.10	1.04	0.42		25	72.0	3.88	1.83
IG8	0.83	3.66		6.17	10.40	4.85	1.00	0.24	0.12	0.39	0.05	0.65	0.20		20	65.0	2.62	1.77
IG9*B	0.53	10.30	56.50	11.00	20.20		1.60	0.34	0.20	0.68	0.10	1.37	0.43		32	46.9	4.45	2.58
IG10*	0.72	7.32	47.50	9.19	17.30		1.39	0.29	0.19	0.61	0.09	1.07	0.28	1.28	5	400.0	3.56	2.99
IG11*C	1.50	9.70	65.80	11.10	22.30	8.53	1.56	0.35	0.20	0.71	0.10	1.34	0.46	1.45	11	136.4	4.37	2.20
IG12	1.43	0.80		3.64	5.57		0.61	0.14	0.11	0.22	0.03	0.21			2	800.0	1.18	2.38
IG13	1.31	1.30		4.43	6.50		0.65	0.18	0.12	0.30	0.04	0.23			13	138.5	1.20	2.77
IG14*D2	0.84	11.20	79.10	12.90	23.90		1.82	0.42	0.23	0.75	0.11	1.40	0.49	1.59	20	100.0	4.62	2.49
IG15	0.97	3.35		8.84	17.40		1.48	0.35	0.20	0.56	0.08	0.67	0.16				2.98	3.38
IG16*E	0.44	11.10	73.50	12.40	21.70	10.30	2.18	0.40	0.24	0.82	0.12	1.53	0.53		18	83.3	4.68	2.42
IG17*E	0.28	11.90	67.00	12.90	22.60	10.70	1.93	0.39	0.12	0.82	0.12	1.46	0.48	1.84	26	42.3	4.90	1.95
IG18*F	0.41	8.84	59.80	11.10	18.80	8.53	1.76	0.37	0.19	0.65	0.10	1.23	0.41		28	46.4	4.00	1.64
IG19	0.14	5.02	44.00	8.23	13.30	7.11	1.28	0.30	0.14	0.51	0.07	0.87	0.26		23	87.0	2.93	2.43
IG20*G1	0.55	7.72	62.50	10.10	16.80		1.57	0.32	0.17	0.55	0.08	1.14	0.31		10	200.0	3.71	1.85
IG21*G2	0.32	8.36	50.40	9.51	17.20	7.46	1.42	0.31	0.21	0.66	0.09	0.97	0.36		15	100.0	3.55	1.62
IG22	0.67	3.80	33.70	6.55	13.10		0.97	0.24	0.13	0.38	0.05	0.45	0.14		20	75.0	2.36	2.69
error (mean%)	12.5	4.5	38.2	2.8	6.7	33.4	9.1	4.3	22.5	6.5	25.0	8.1	12.1	31.8		129.6	2.6	9.3
error (range %)	4.4--30	2--13	32--49	2.2-4.5	2.4-13	22-44	3.2-40	3.4-5.5	14-39	4.4-10	11-42	3.4-48	7-25	22-44		14.3-800	1.2-3.5	1.6-19

Tabel 2. Correlation coefficients of trace elements in 22 samples listed in Table 1.

	Na	K	Ca	Sc	Cr	Fe	Co	Zn	As	Se	Br	Rb	Sr	Zr	Sb	Cs	Ba	La	Ce	Nd	Sm	Eu	Tb	Yb	Lu	Hf	Ta	Ir	Th	U
Na	1.00																													
K	0.40	1.00																												
Ca	-0.85	-0.34	1.00																											
Sc	0.95	0.38	-0.92	1.00																										
Cr	0.92	0.31	-0.89	0.98	1.00																									
Fe	0.89	0.32	-0.92	0.95	0.94	1.00																								
Co	0.75	0.35	-0.79	0.79	0.71	0.85	1.00																							
Zn	0.66	0.12	-0.92	0.75	0.70	0.76	0.59	1.00																						
As	0.00	-0.37	-0.08	0.01	0.10	0.27	0.08	-0.03	1.00																					
Se	-0.37	-0.53	-0.62	-0.16	-0.13	-0.22	-0.46	0.85	0.01	1.00																				
Br	0.90	0.29	-0.73	0.84	0.79	0.73	0.62	0.66	-0.12	-0.12	1.00																			
Rb	0.95	0.40	-0.92	1.00	0.98	0.95	0.79	0.75	0.00	-0.17	0.83	1.00																		
Sr	0.98	0.36	-0.79	0.91	0.88	0.83	0.71	0.60	-0.06	-0.48	0.91	0.91	1.00																	
Zr	0.88	0.80	-0.74	0.90	0.89	0.84	0.69	0.42	-0.54	-0.96	0.79	0.89	0.87	1.00																
Sb	0.00	-0.22	-0.02	0.05	0.12	0.20	0.07	0.08	0.60	-0.34	-0.13	0.03	-0.06	-0.36	1.00															
Cs	0.95	0.39	-0.92	1.00	0.98	0.93	0.78	0.76	-0.02	-0.09	0.85	1.00	0.91	0.90	0.02	1.00														
Ba	0.75	0.87	-0.77	0.87	0.71	0.84	0.77	0.50	-0.30	-0.21	0.43	0.87	0.59	0.58	0.19	0.86	1.00													
La	0.95	0.35	-0.92	0.98	0.94	0.95	0.84	0.76	0.08	-0.35	0.83	0.97	0.92	0.86	0.10	0.97	0.94	1.00												
Ce	0.93	0.35	-0.90	0.96	0.94	0.95	0.83	0.74	0.15	-0.36	0.81	0.96	0.89	0.84	0.15	0.96	0.91	0.99	1.00											
Nd	0.84	0.94	-0.64	0.95	0.79	0.70	0.80	0.36	-0.68	-0.60	0.67	0.96	0.78	0.92	-0.17	0.95	0.89	0.98	0.92	1.00										
Sm	0.94	0.31	-0.89	0.95	0.90	0.94	0.88	0.73	0.07	-0.49	0.81	0.95	0.91	0.85	0.08	0.95	0.88	0.99	0.97	0.95	1.00									
Eu	0.92	0.31	-0.89	0.93	0.88	0.93	0.86	0.75	0.14	-0.45	0.79	0.92	0.88	0.80	0.14	0.92	0.97	0.99	0.98	0.97	0.98	1.00								
Tb	0.77	0.19	-0.84	0.84	0.84	0.90	0.77	0.69	0.32	0.13	0.57	0.83	0.70	0.53	0.31	0.83	0.61	0.89	0.90	0.37	0.89	0.90	1.00							
Yb	0.94	0.33	-0.91	0.97	0.94	0.94	0.83	0.72	0.05	-0.27	0.83	0.97	0.91	0.90	0.09	0.97	0.83	0.99	0.98	0.96	0.98	0.97	0.89	1.00						
Lu	0.95	0.34	-0.91	0.98	0.95	0.94	0.83	0.73	0.04	-0.29	0.84	0.98	0.92	0.91	0.08	0.98	0.83	0.99	0.98	0.98	0.98	0.96	0.87	1.00	1.00					
Hf	0.97	0.39	-0.90	0.99	0.95	0.93	0.81	0.71	0.00	-0.29	0.82	0.98	0.93	0.84	0.05	0.98	0.90	0.98	0.97	0.96	0.97	0.95	0.85	0.97	0.98	1.00				
Ta	0.89	0.89	-0.83	0.98	0.94	0.86	0.59	0.55	-0.48	-0.16	0.67	0.97	0.80	0.90	0.07	0.98	0.85	0.93	0.89	0.94	0.89	0.83	0.68	0.93	0.95	0.96	1.00			
Ir	0.32	0.06	-0.29	0.31	0.33	0.17	0.07	0.15	-0.32	-0.01	0.39	0.32	0.35	0.60	-0.51	0.34	0.05	0.22	0.17	0.15	0.18	0.16	-0.02	0.21	0.24	0.27	0.35	1.00		
Th	0.97	0.33	-0.91	0.98	0.96	0.95	0.81	0.74	0.09	-0.33	0.84	0.98	0.93	0.88	0.10	0.98	0.88	0.99	0.99	0.96	0.98	0.97	0.88	0.99	0.99	0.99	0.95	0.25	1.00	
U	0.07	-0.19	-0.10	0.11	0.11	0.22	0.33	-0.03	0.44	-0.34	-0.10	0.10	0.02	-0.40	0.47	0.09	-0.21	0.25	0.30	0.31	0.26	0.32	0.42	0.23	0.20	0.15	-0.29	-0.40	0.21	1.00
CaCO3	-0.87	-0.32	0.98	-0.94	-0.90	-0.90	-0.77	-0.92	-0.02	-0.58	-0.80	-0.94	-0.83	-0.76	0.05	-0.94	-0.71	-0.93	-0.92	-0.74	-0.91	-0.89	-0.82	-0.92	-0.93	-0.91	-0.82	-0.3	-0.93	-0.08

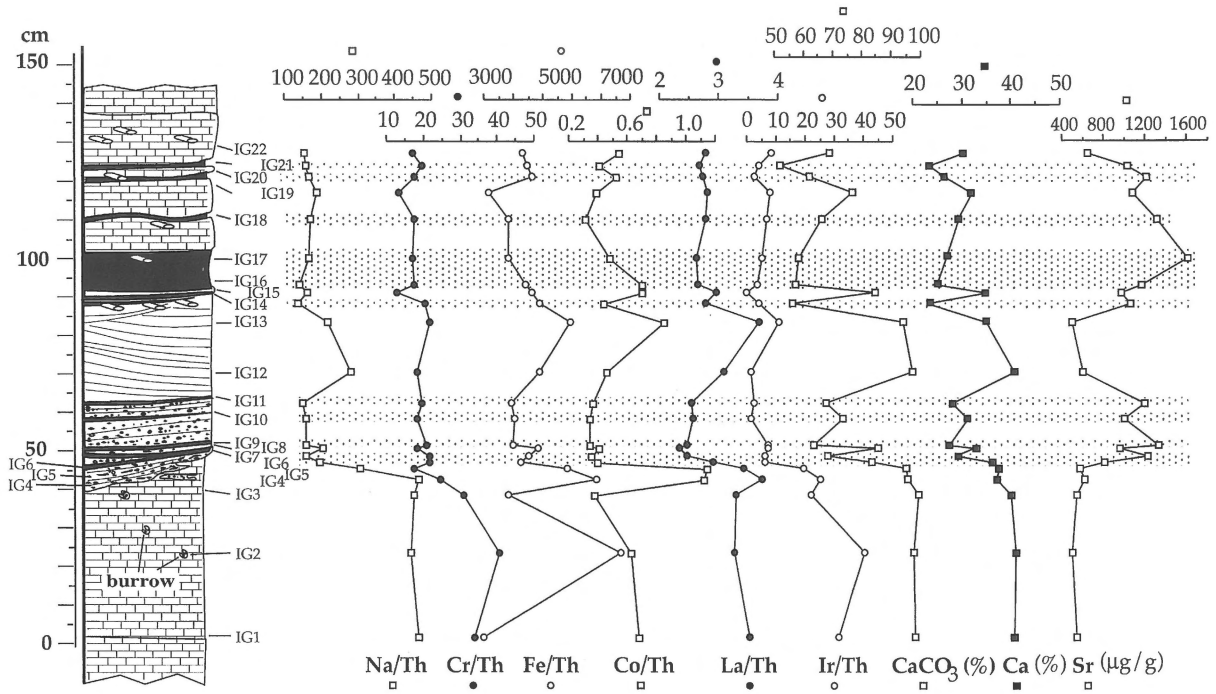

Figure 1. Thorium-normalized profiles of trace elements measured across the K/T boundary in the Geulhemmerberg section, 7 km ENE of Maastricht (see Brinkhuis and Smit, this issue, for full locality details). $CaCO_3$ content is measured separately. The K/T boundary is located between samples IG3 and 4. Values in stippled areas are from clay layers. Values of Ca and $CaCO_3$ are in %, Sr in μg/g.

Discussion

Siderophile elements (Cr, Fe, Co, Ni, Ir)

The group of siderophile trace elements shows high concentrations in extraterrestrial material in comparison with the average composition of the continental crust. The group is thus expected to be enriched at the K/T boundary. However, Fe and Co are usually enriched in iron encrustations, such as those present in hardgrounds, and in pyrite, both of which are often present at the K/T boundary. Also, siderophile elements, with the exception of the Pt-group elements, are mobile in different diagenetic environments. Schmitz et al. (1988) have argued that many siderophile elements will precipitate on lithologic discontinuities, such as hardgrounds and the K/T boundary layer, due to differences in Ph and Eh conditions, irrespective of whether these elements are cosmically derived or not. Previous analyses of a millimetre-thin iron-encrusted ash layer in Miocene sediments in Crete, Greece (G. Klaver and F. Bianchi, personal communication), have shown that the siderophile elements Fe, Co and Ni indeed do precipitate on such layers, but that Ir does not. In K/T boundary profiles without a lithologic discontinuity such as at DSDP sites 524 and 577 (Michel et al. 1985), only Ir and Cr have anomalous high concentrations. In effect, Cr, like Ir, is invariably anomalously enriched at the K/T boundary, and is probably also derived from a cosmic source (e.g. Smit and Ten Kate 1982).

In the Geulhemmerberg section, Co and Fe are slightly enriched near the Berg en Terblijt hardground (samples IG4 and 5; Figure 1, Table 1). This enrichment is most probably due to iron-oxide encrustation. Neither Ir nor Cr shows a significant enrichment in the clay layers. However, the Th-normalized values of Cr and Ir below the hardground (samples IG1–3) are two and six times higher than the respective averages of the other samples. It is not clear whether the high normalized values are an artifact of the normalization, or whether they are due to downward diffusion or transport of Ir and Cr from a once-present, but later removed Ir-rich impact-ejecta deposit. Because Ir and Cr are not enriched in samples IG12 and 13, which have the same carbonate content and lithology as the upper-

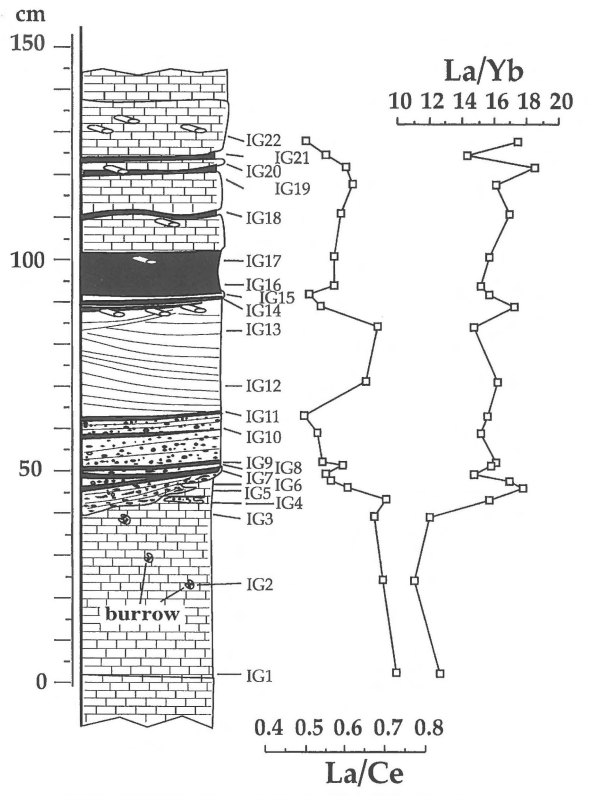

Figure 2. Profiles of La/Ce and La/Yb ratios across the K/T boundary in the Geulhemmerberg section.

most Maastrichtian samples IG1 to 3, and also because downward diffusion of Ir has been demonstrated by Rocchia (Rocchia et al. 1987) in other K/T sections with an Ir anomaly, downward diffusion remains a possibility, betraying possibly an eroded Ir anomaly in the Geulhemmerberg section. Future more detailed analyses may resolve this problem.

Chalcophile elements (Co, Zn, As, Se, Sb)

Chalcophile elements are often precipitated in sulphides, under anoxic conditions. They occur in high concentrations in anoxic shales such as the Bonarelli level at the Cenomanian/Turonian boundary in the Italian Apennines and in the Permian Kupferschiefer in Poland (Kuch and Von Gruenewaldt 1982). At the K/T boundary, Co, As, Zn and Sb concentrations are anomalously high in those sections which show a strong lithologic contrast and a well-preserved K/T boundary ejecta layer. Also, chalcophile elements precipitate at lithologic discontinuities, such as the Miocene ash layer mentioned above. Well-preserved K/T boundary sequences show evidence of a short period of anoxia at the boundary, like organic-rich sediments (Stevns Klint, Denmark; Schmitz et al. 1988) or abundant pyrite (Zumaya, Spain; Smit 1990). Although organic compounds are extremely well preserved in the clay layers at Geulhemmerberg (Yamamoto et al., this issue), the organic-C content is not particularly high. Like Ir and Cr, As and Sb appear slightly enriched in the samples below and at the K/T boundary (IG1 to 5), but, in contrast to Cr and Ir, also in the carbonate-rich interval in samples IG12 and 13 (Figure 1).

Lithophile elements (Sc, REE, Hf, Ta, Th)

The lithophile elements strongly correlate with the insoluble residue in the Geulhemmerberg section (Table 2), and as observed earlier, also in other K/T boundary sequences (Smit and Ten Kate 1982).

The REE profiles show interesting, but not easily explained results. Previous analyses of pelagic carbonate sequences such as DSDP site 577 (Michel et al., 1985) have shown that REE are strongly absorbed on pelagic carbonate, retaining the negative Ce anomaly of Pacific Ocean water. On the other hand, REE are usually also enriched in the clay fraction (Smit and Ten Kate 1982). The REE concentrations in an alternation of almost pure limestones and clay layers such as in the Geulhemmerberg section may be a balance between precipitation on carbonate and increased clay content. The Th-normalized REE concentrations in the limestones are slightly enriched with respect to the clay layers, indicating precipitation from seawater on carbonate particles. Interesting, in this respect, is the La/Ce ratio (Figure 2). Cerium appears to be slightly enriched in the clay layers, indicating dysoxic conditions in seawater during the deposition of these layers. The La/Yb ratio is lower below the Berg en Terblijt hardground, mainly due to higher La values above the hardground. This may indicate a change in the source rocks of the insoluble residue fraction, beginning at the K/T boundary.

Other trace elements

The profiles of the other trace elements are not easily interpreted. The U/Th ratio is higher in the limestones than in the clay layers. The Sr distribution is noteworthy. Usually, Sr has a high positive correlation coefficient with Ca (e.g. r = 0.8; Smit and Ten Kate 1982) because both elements belong to the same group 2 of

the periodic table. However, in the Geulhemmerberg profile, Sr correlates strongly negatively (r = – 0.793, Table 2) with $CaCO_3$ and Ca. Because the Sr concentrations are relatively low in the limestones with respect to Sr concentrations known from limestones elsewhere, the negative correlation is probably due to the leaching of Sr from porous limestones, and probably indicates that the clay layers are shielded from diagenesis (Vonhof and Smit, this issue).

Conclusions

1) The analysis by INAA of elemental concentrations in the Geulhemmerberg section did not yield a clear Ir anomaly at the K/T boundary.
2) The Ir/Th and Cr/Th ratios appear to be slightly higher in the uppermost Maastrichtian, possibly due to downward diffusion, or transport, of Ir from a once-present ejecta deposit.
3) Strontium concentrations are higher in the clay layers than in the limestone layers. This leads to a negative correlation between Ca and Sr, and is probably due to leaching of Sr from the porous carbonate rocks.
4) Low La/Ce ratios in the clay layers indicate dysoxic seawater during the deposition of the clays.
5) A change-over from low La/Yb ratios in the Maastrichtian to high La/Yb ratios in the Danian may reflect a change in the source rocks of the clay minerals.

This is contribution 941204 of the Netherlands Research School of Sedimentary Geology (NSG).

References

Alvarez, W. & F. Asaro 1990 What caused the mass extinction? An extraterrestrial impact – Sci. American 263: 78–84

Alvarez, L.W., W. Alvarez, F. Asaro & H.V. Michel 1980 Extraterrestrial cause for the Cretaceous-Tertiary extinction – Science 208: 1095–1108

Brinkhuis, H. & J. Smit (this issue) The Geulhemmerberg Cretaceous/Tertiary boundary section (Maastrichtian type area, SE Netherlands); an introduction

Kucha, H. & G. von Gruenewaldt 1982 Platinum-group metals in the Zechstein copper deposits, Poland – Econ. Geol. and Bull. Soc. Econ. Geol. 77: 1578–1591

Michel, H.V., F. Asaro, W. Alvarez & L.W. Alvarez 1985 Elemental profile of iridium and other elements near the Cretaceous/Tertiary boundary in Hole 577B. In: G.R. Heath & L.H. Burckle (eds): Initial Reports of the Deep-Sea Drilling Project 86, U.S. Gov. Printing Office, Washington D.C.: 533–538

Rocchia, R., D. Boclet, P. Bonté, J. Devineau, C. Jéhanno & M. Renard 1987 Comparaison des distributions de l'iridium observées à la limite Crétacé-Tertiaire dans divers sites européens – Mém. Soc. Géol. France, N.S. 150: 95–103

Rocchia, R., D. Boclet, P. Bonté, C. Jéhanno, Y. Chen, V. Courtillot, C. Mary & F. Wezel 1990 The Cretaceous-Tertiary boundary at Gubbio revisited: vertical extent of the Ir anomaly – Earth Planet. Sci. Lett. 99: 206–219

Schmitz, B., P. Andersson & J. Dahl 1988 Iridium, sulfur isotopes and rare earth elements in the Cretaceous-Tertiary boundary clay at Stevns Klint, Denmark – Geochim. Cosmochim. Acta 52: 229–236

Smit J. 1990 Meteorite impact, extinctions and the Cretaceous-Tertiary boundary – Geol. Mijnbouw 69: 187–204

Smit, J. & J. Hertogen 1980 An extraterrestrial event at the Cretaceous-Tertiary boundary – Nature 285: 198–200

Smit, J. & W.G.H.Z. ten Kate 1982 Trace element patterns at the Cretaceous-Tertiary boundary – consequences of a large impact – Cretaceous Research 3: 307–332

Vonhof, H.B. & J. Smit (this issue) Strontium-isotope stratigraphy of the type Maastrichtian and the Cretaceous/Tertiary boundary in the Maastricht area (SE Netherlands)

Yamamoto, M., K. Ficken, M. Baas, H.-J. Bosch & J.W. de Leeuw (this issue) Molecular palaeontology of the earliest Danian at Geulhemmerberg (the Netherlands)